An Analysis of an Electric Wall Type Cavity Resonator for Concentric Array Radial Line Slot Antennas

Tatsuya Yamamoto Jiro Hirokawa Makoto Ando Naohisa Goto
Dept. of Electrical and Electronic Eng.,
Tokyo Institute of Technology
2-12-1 Ookayama, Meguro-ku, Tokyo 152, Japan

1. INTRODUCTION

In this paper, we analyzed an electric wall type cavity resonator for the excitation of a rotating mode in the concentric array radial line slot antennas (CA-RLSA)[1]. The cavity resonator is excited by a feed pin and is perturbed by a parasitic pin. Then it radiates a rotating mode with the dependence of exp (jφ) in the φ-direction in a radial waveguide. It enables concentric arrangement of slots in RLSA and enhances the rotationally symmetry of the operation. However, it was difficult to design to get good symmetry by experiments. So the optimization based on the analysis is indispensable. By using mode matching technique, we can predict the input impedance of the feed pin and the field distribution in the radial waveguide. Especially the analysis simulates well the φ-variation of the inner field with a 10dB ripple.

2. MODE MATCHING ANALYSIS [2]

An analysis model is shown in Figure 2. First we consider fields excited by a single current J_i, i=1 for a feed pin or i=2 for a parasitic pin. The electric current

$$J_i = I_i \hat{z}\delta(\varphi - \varphi_i)\sin\left\{\frac{\pi}{2l_i}(z-(d-l_i))\right\} \quad (i = 1, 2) \qquad \cdots\cdots(1)$$

is assumed on the pin #i. Electric field in each region is expanded in terms of TM modes.

Region I

$$E_{z\,I} = \sum_n \sum_m A_{nm} J_n(k_{\rho I}\rho)\cos n\varphi \cos\frac{m\pi}{d} z \qquad \cdots\cdots(2)$$

Region II

$$E_{z\,II} = \sum_n \sum_m \left\{B_{nm} J_n(k_{\rho II}\rho) + C_{nm} H_n(k_{\rho II}\rho)\right\}\cos n\varphi \cos\frac{m\pi}{d} z \qquad \cdots\cdots(3)$$

Region III

$$E_{z\,III} = \sum_n \sum_m \left\{D_{nm} J_n(k_{\rho III}\rho) + F_{nm} H_n(k_{\rho III}\rho)\right\}\cos n\varphi \cos\frac{m\pi}{g} z \qquad \cdots\cdots(4)$$

Region IV

$$E_{zIV} = \sum_n \sum_m G_{nm} H_n(k_{\rho IV}\rho)\cos n\varphi \cos\frac{m\pi}{h} z \quad \cdots\cdots(5)$$

where k_ρ satisfy the following equations.

$$\begin{cases} k_{\rho I}{}^2 + \left(\frac{m\pi}{d}\right)^2 = \varepsilon_{\ I}\, k_0{}^2 \ , \ k_{\rho II}{}^2 + \left(\frac{m\pi}{d}\right)^2 = \varepsilon_{\ II}\, k_0{}^2 \\ k_{\rho III}{}^2 + \left(\frac{m\pi}{g}\right)^2 = \varepsilon_{\ III}\, k_0{}^2 \ , \ k_{\rho IV}{}^2 + \left(\frac{m\pi}{h}\right)^2 = \varepsilon_{\ IV}\, k_0{}^2 \end{cases} \quad \cdots\cdots(6)$$

The φ-component of the magnetic field in each region is derived from

$$H_\varphi = -\frac{j\omega\varepsilon_r}{k_\rho}\frac{\partial E_z}{\partial \rho} \quad \cdots\cdots(7)$$

The unknown coefficients $A_{nm} \sim G_{nm}$ in eqs. (2)~(5) will be determined by imposing the following boundary conditions multiplied with appropriate weighting functions at three discontinuities.

(i) Boundary condition at $\rho = b_i$

$$\begin{cases} \int_0^{2\pi} b_i \int_0^d E_{z\,I}\ \cos n'\varphi \cos\frac{m'\pi}{d} z dz d\varphi = \int_0^{2\pi} b_i \int_0^d E_{z\,II}\ \cos n'\varphi \cos\frac{m'\pi}{d} z dz d\varphi \\ \int_0^{2\pi} b_i \int_0^d (H_{\varphi II} - H_{\varphi I})\cos n'\varphi \cos\frac{m'\pi}{d} z dz d\varphi = \int_0^{2\pi} b_i \int_{d-l_i}^d J_i \cos n'\varphi \cos\frac{m'\pi}{d} z dz d\varphi \end{cases} \quad \cdots\cdots(8)$$

(ii) Boundary condition at $\rho = a$

$$\begin{cases} \frac{1}{d}\int_0^{2\pi} a \int_0^d E_{z\,II}\ \cos n'\varphi \cos\frac{m'\pi}{d} z dz d\varphi = \frac{1}{d}\int_0^{2\pi} a \int_0^g E_{z\,III}\ \cos n'\varphi \cos\frac{m'\pi}{d} z dz d\varphi \\ \frac{1}{g}\int_0^{2\pi} a \int_0^g H_{\varphi\,II}\ \cos n'\varphi \cos\frac{m'\pi}{g} z dz d\varphi = \frac{1}{g}\int_0^{2\pi} b \int_0^g H_{\varphi\,III}\ \cos n'\varphi \cos\frac{m'\pi}{g} z dz d\varphi \end{cases} \quad \cdots\cdots(9)$$

(iii) Boundary condition at $\rho = a + c$

$$\begin{cases} \frac{1}{h}\int_0^{2\pi} (a+c) \int_0^g E_{z\,III}\ \cos n'\varphi \cos\frac{m'\pi}{h} z dz d\varphi = \frac{1}{h}\int_0^{2\pi} (a+c) \int_0^h E_{z\,IV}\ \cos n'\varphi \cos\frac{m'\pi}{h} z dz d\varphi \\ \frac{1}{g}\int_0^{2\pi} (a+c) \int_0^g H_{\varphi\,III}\ \cos n'\varphi \cos\frac{m'\pi}{g} z dz d\varphi = \frac{1}{g}\int_0^{2\pi} (a+c) \int_0^g H_{\varphi\,IV}\ \cos n'\varphi \cos\frac{m'\pi}{g} z dz d\varphi \end{cases} \quad (10)$$

By solving a set of integral eqs. (8)~(10) for $A_{nm} \sim G_{nm}$, we can obtain the field distribution in the radial waveguide produced from the single currents J_i (i=1 or 2).

Next, the ratio of two currents of I_1 and I_2 is determined by the electromotive force method (EFM). In EFM, the self and mutual impedances of the electric currents on the two pins are defined by

$$Z_{ij} = -\frac{1}{I_i^* I_j} \int_{d-l_i}^d \mathbf{J}_i \cdot \mathbf{E}_i(J_j) dz \quad \cdots\cdots(11)$$

Where $\mathbf{E}_i(J_j)$ is the electric field produced from the current J_j.

The following matrix expression

$$\begin{bmatrix} V_1 \\ 0 \end{bmatrix} = \begin{bmatrix} Z_{11} & Z_{12} \\ Z_{21} & Z_{22} \end{bmatrix} \begin{bmatrix} I_1 \\ I_2 \end{bmatrix} \quad \cdots\cdots(12)$$

is satisfied by using the above impedances when the feed pin is excited by a voltage of V_1 and the parasitic pin is shorted ($V_2 = 0$). The input impedance at the feed point as well as the ratio of I_1 / I_2 is obtained

$$Z_{in} = \frac{V_1}{I_1} = Z_{11} - \frac{Z_{12}Z_{21}}{Z_{22}} \quad \text{.....(13)}$$

$$\frac{I_2}{I_1} = -\frac{Z_{21}}{Z_{22}} \quad \text{.....(14)}$$

The field distribution in the radial waveguide is expressed as superposition of the two fields in eq. (5) produced from the currents J_1 and J_2 on the feed and the parasitic pin respectively with the ratio given in (14).

3. RESULT

A feed circuit is fabricated. The parameters are listed on Table 1. The frequency dependence of the input impedance is shown in Figure 3. The agreement between the calculated and the measured result are fairly good. The amplitude distribution measured along the circumference direction of the radial waveguide is shown in Figure 4. The field is calculated and measured at a distance of 5λ from the center of the radial waveguide. The analysis reasonably predict the φ-variation of the inner field with a 10dB ripple.

4. CONCLUSION

In this paper, we analyzed an electric wall type cavity resonator for CA-RLSA using mode matching technique. We fabricated a feed circuit and compared calculated results with measured results. As for the input impedance, the agreement between the calculated and the measured result are fairly good. Moreover field distribution in the radial waveguide with a 10dB ripple is well simulated by the analysis. It is a future problem to optimize parameters and to realize the perfect rotating mode.

REFERENCES

[1] Hosono,S., Hirokawa,J., Ando,M., Goto,N., Arai,H., "A Rotating Mode Radial Line Slot Antenna Fed by a Cavity Resonator", IEICE Trans. on Commun., Vol.E78-B, No.3, PP.407-413, March 1995

[2] Ueda,H., Arai,H., Goto,N., "Magnetic wall type resonator for Radial Line Slot Antenna", Technical Report., IEICE Japan, AP94-115, 1995-1

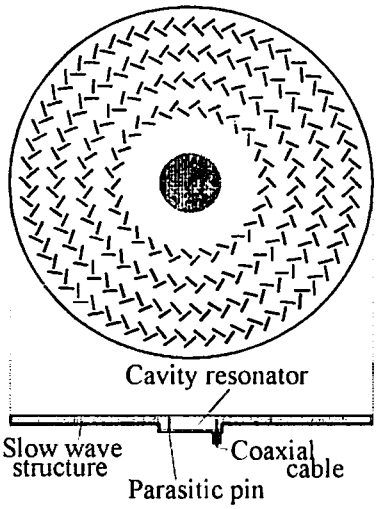

Figure 1. Concentric array RLSA

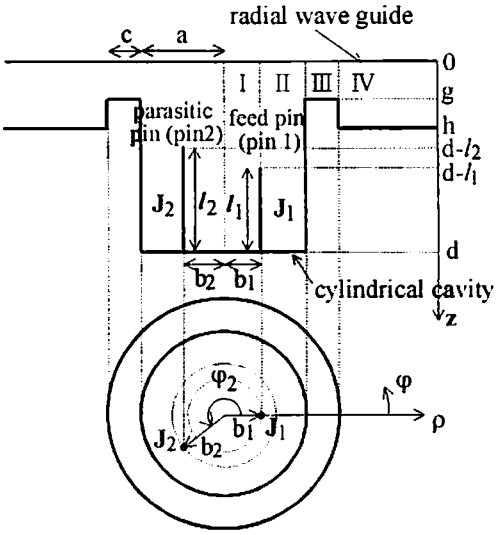

Figure 2. An analysis model

Table 1. Design parameters

Design frequency f	11.85[GHz]	Length of parasitic pin l_2	4.3[mm]
Radius of a cavity a	15.0[mm]	Height of a gap g	1.5[mm]
Location of feed pin b_1	7.3[mm]	Height of a radial waveguide h	3.0[mm]
Location of parasitic pin b_2	7.3[mm]	Height of a cavity d	7.3[mm]
Angle between the feed and parasitic pins φ_2	225[deg]	Relative permittivity $\varepsilon_{\mathrm{I}}, \varepsilon_{\mathrm{II}}, \varepsilon_{\mathrm{III}}$	1.0
Wall thickness c	4.0[mm]	Relative permittivity $\varepsilon_{\mathrm{IV}}$	1.17
Length of feed pin l_1	5.4[mm]		

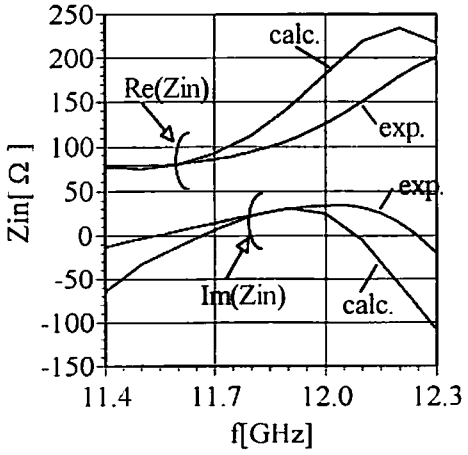

Figure 3. Input impedance peculiarity

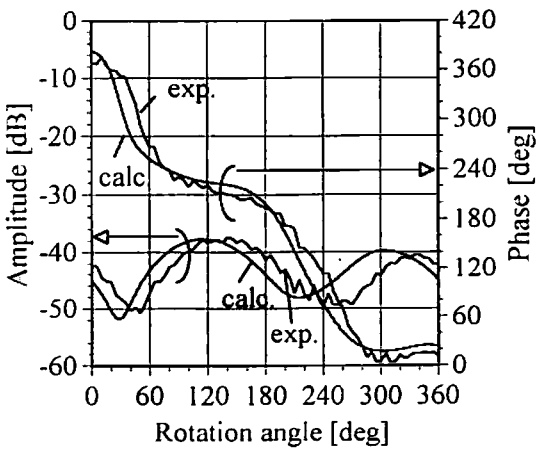

Figure 4. Field distribution along the circumference direction